

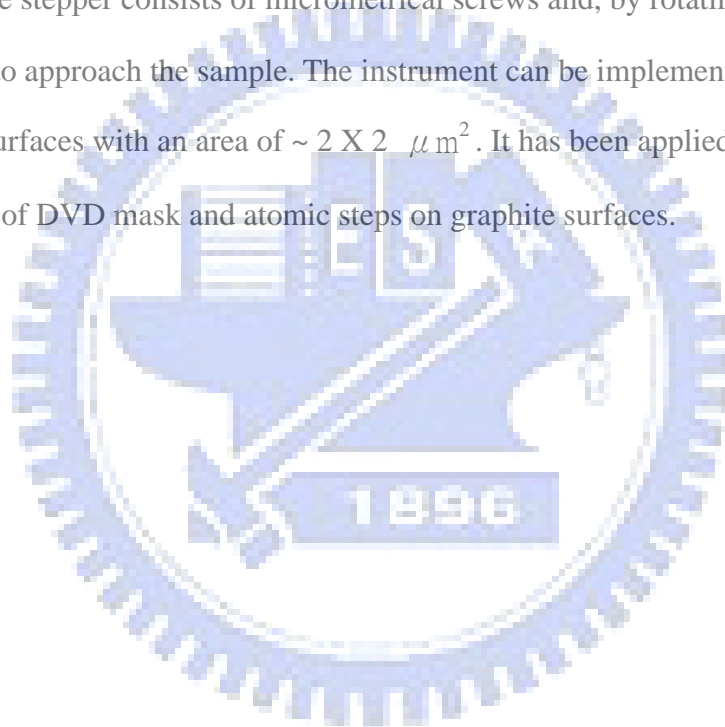
摘要

掃瞄穿隧顯微鏡已經發展了二十餘年了，它給予了我們奈米世界的新視野，而且也真實地應用到量子力學的理论(穿隧效應)。它在研究表面科學時的重要性已經是眾所周知的，然而它的價格和複雜度仍然阻礙著大學部以下的學生去使用來研究奈米科學。所以我們組裝了一台簡易 STM，用便宜的蜂鳴片來當掃瞄頭，而且不需用高壓電路來驅動。步進器則使用幾根測微螺絲，再利用槓桿原理，用手去轉動就可以把探針接近樣品到奈米的距離。我們的儀器可以掃出 $2 \times 2 \mu\text{m}^2$ 大小的面積，而且可以掃到石墨表面的台階還有 DVD 光碟上的紋路。



Abstract

Scanning Tunneling Microscopy (STM) has been developed for more than 20 years. It brought us a new tool to explore the nano world even on atomic scale and it also presented us the application of quantum mechanics (tunneling effect). Its importance in research of surface science has been well established, but its high cost and complexity prohibit undergraduate students from studies by using this tool. We build a simple STM using low cost audio transducers for STM scanner and low voltage for driving it. The stepper consists of micrometrical screws and, by rotating the screws, it drive the tip to approach the sample. The instrument can be implemented to scan conducting surfaces with an area of $\sim 2 \times 2 \mu\text{m}^2$. It has been applied to obtain the STM images of DVD mask and atomic steps on graphite surfaces.



致謝

時光飛逝，兩年的時間一下就過了。想當初剛進實驗室的我，在對一切懵然無知的情形下，於實驗上遭遇了很多挫折，但在簡紋濱老師耐心的指導下，最後實驗終於能有點成果出來，在此特別感謝簡老師。另外也要感謝歐逸青學長的指點，讓我的實驗能夠更順利。也感謝林彥甫和廖泰慶同學，很多實驗上的問題也是和你們討論過後，才比較會有心得。除此之外，也感謝邱亦正和吳俊吉學弟，有了他們的幫忙，我的研究才可以更快完成。還有郭融學整理的資料對我完成論文很有幫助，以及陳建翔很辛苦地幫我們處理報帳問題，也要感謝他們。另外我也從陳怡然身上得到很多他對事物的獨特看法，實在令人耳目一新。還有傅勝凱為實驗室傳達了上帝的福音，也為實驗室增添了一些神跡。當然還有聽說笑點很低的 Acer，和專為實驗室出遊及聚餐出謀劃策的侯朝振，還有差點被忽略的洪祥智也是要好好地感謝他們的辛勞。綜合以上所述，實在感覺出之於己者太少，得之於人者太多，有了這群伙伴，我才能在實驗遇到挫折時，愈挫愈勇。

Lists of figures

- Fig. 2.1.** The one-dimensional barrier potential model.
- Fig. 2.2.** The one-dimensional metal-vacuum-metal tunneling junction.
- Fig. 2.3.** The Curie's experiment.
- Fig. 2.4.** The experiment of the inverse piezoelectric effect.
- Fig. 2.5.** Definition of the piezoelectric coefficients.
- Fig.2.7.** The tube scanner.
- Fig.2.8.** The tube bends by applying a voltage.
- Fig. 2.9.** The image of scanning a DVD master.
- Fig. 2.10.** The constant current mode.
- Fig.2.11.** The constant height mode.
- Fig. 3.1** The audio transducer.
- Fig. 3.2.** The disk bows up.
- Fig 3.3.** The disk bows down.
- Fig. 3.4.** The electrode is divided into four quadrants.
- Fig. 3.5.** The X -scanning.
- Fig.3.6.** The tip holder
- Fig.3.7.** The scanner holder
- Fig.3.8.** The disk scanner
- Fig. 3.9.** The sample stage.
- Fig.3.10.** Electrochemical etching of tungsten or gold tips.
- Fig. 3.11.** The SEM images of a W tip.
- Fig.3.12** The STM frame.

- Fig.3.13** The 1/4"-80 fine adjustment screw.
- Fig.3.14.** The conceptual diagram of Z-axis feedback system in STM.
- Fig.3.15.** The whole electronic elements of our STM.
- Fig.3.16.** The current to voltage amplifier.
- Fig.3.17.** The current amplifier we use.
- Fig.3.18.** The feedback loop circuit.
- Fig.3.19.** The negative absolute circuit.
- Fig.3.20.** X Y Z position.
- Fig.3.21.** The D/A converters.
- Fig.3.22.** The A/D converter.
- Fig.3.23.** The STM control program.
- Fig.3.24.** The NIP program.
- Fig.4.1.** The mass, spring, and damper system.
- Fig.4.2** The graphite image with 2 steps in the area.
- Fig.4.3.** The more amplification image of Fig.4.3.
- Fig.4.4** A series of scanning images of graphite.
- Fig.4.5.** The topography of DVD master surface taken by the commercial SPM in our laboratory.
- Fig.4.6.** The data analysis of Fig.4.5..
- Fig.4.7** The image of DVD master surface taken by our simple STM.
- Fig.4.8.** The image is taken in smaller scan area which means higher amplification.

Contents

Chinese abstract.....	i
English abstract.....	ii
Acknowledgement	iii
Lists of figures.....	iv
Contents	vi
Chapter 1 Introduction.....	1
Chapter 2 Scanning Tunneling Microscope.....	2
2.1 Tunneling effect.....	2
2.2 Piezoelectric effect.....	4
2.3 Scanning tunneling microscope.....	7
Chapter 3 Experiments.....	13
3.1 Mechanical part.....	13
3.1.1 Disk scanner.....	13
3.1.2 Sample stage.....	17
3.1.3 Tip.....	17
3.1.4 Vibration isolation system.....	21
3.1.5 The STM frame and the stepper.....	21
3.2 Electronic part.....	22
3.2.1 Current amplifier.....	24
3.2.2 Feedback loop.....	25
3.2.3 Negative absolute circuit.....	25
3.2.4 X-Y-Z position.....	26
3.2.5 Digital to analog circuit.....	27
3.2.6 Analog to digital circuit.....	28
3.3 Computer part.....	29
Chapter 4 Results and Discussions.....	31
4.1 Spring vibration isolation system.....	31
4.2 Test for designing the feedback loop	32
4.3 STM images.....	33
4.4 Calibration.....	35
Chapter 5 Conclusion.....	38
Reference	39

Chapter 1 Introduction

Learning how to build an instrument for our research is an important thing when we want to improve our performance. An instrument which we build ourselves is not only cheaper but also suits to our requirements. Commercial SPMs are very frequently used in our Nano and Quantum Phenomena Laboratory. If there is something wrong with the elements of SPMs, we would always cost high money to repair them and our experiment would be delayed. A home-made instrument can be low cost if we can replace the commercial instrument by it. Since we have known the principle of STM from our daily works in Laboratory, we try to build a home-made Scanning Tunneling Microscope and hope the experience of doing this will be useful in the future.



Chapter 2 Scanning Tunneling Microscope

2.1 Tunneling effect

In classical mechanics, a particle can not move in the region where the potential of this region is larger than the total energy of the particle. However, the particle has a chance to transmit through a potential barrier higher than its total energy by using the quantum mechanics. We consider a simple one-dimension model for explanation of tunneling effect in the followings. In classical mechanics, a particle with energy E moving in a potential $U(z)$ is described by

$$\frac{p_z^2}{2m} + U(z) = E \quad (2.1)$$

where m is the mass and p_z is the momentum of the particle. The kinetic energy of a classical particle is always a positive value, so the particle can not exist in the region of $E < U(z)$. If we use quantum mechanics, the state of the particle can be described by a wave function, $\psi(z)$, and the corresponding Schrodinger's equation is

$$-\frac{\hbar^2}{2m} \frac{d^2}{dz^2} \psi(z) + U(z)\psi(z) = E\psi(z). \quad (2.2)$$

For a barrier potential case (see Fig. 2.1), in the classically allowed region, Eq. (2.2) has the solution

$$\psi(z) = Ae^{\pm ikz} \quad (2.3)$$

where

$$k = \frac{\sqrt{2m(E-U)}}{\hbar}. \quad (2.4)$$

In the classically forbidden region, Eq. (2.2) has the solution

$$\psi(z) = Ae^{-\kappa z}, \quad (2.5)$$

where

$$\kappa = \frac{\sqrt{2m(U-E)}}{\hbar} \quad (2.6)$$

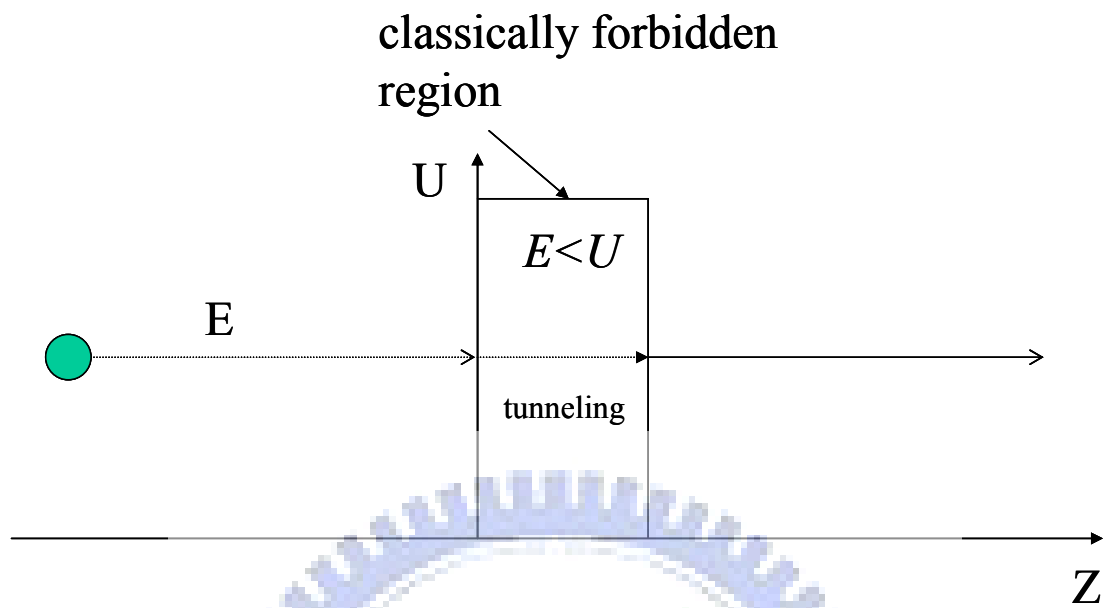


Fig. 2.1 The one-dimensional barrier potential model.

From this theoretical one-dimensional model, we can make qualitative description of the features of metal-vacuum-metal tunneling as shown in Fig. 2.2.

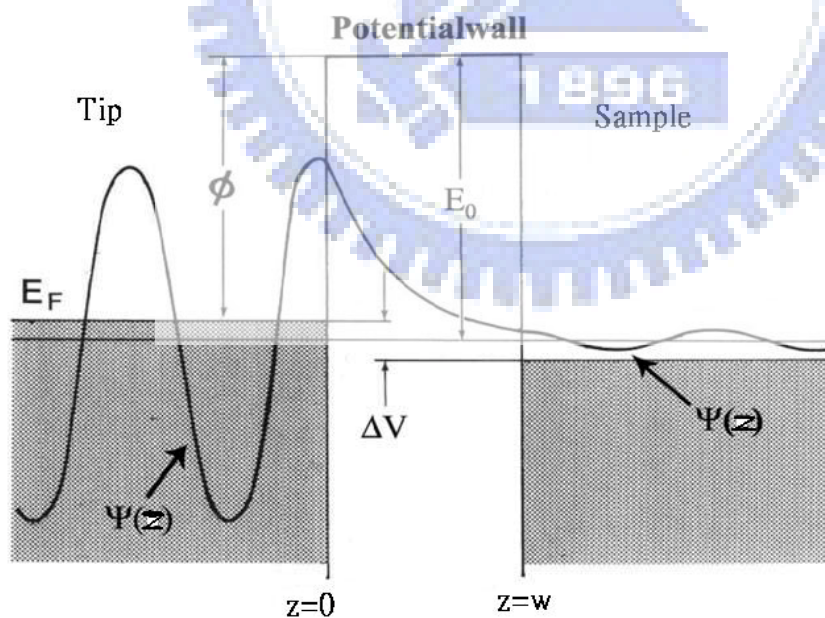


Fig. 2.2. The one-dimensional metal-vacuum-metal tunneling junction. The thermal excitation is neglected here. [1]

To simplify the problem, we assume the work function Φ of the tip and the

specimen are the same. “The work function Φ of the uniform surface of a metal is defined as the difference in potential energy of an electron between the vacuum level and the Fermi level[2]”. In general, the work function depends on what the material is and the orientation of the exposed crystal face. Typical value of the work function of Au or W is about 4-5 eV. The Fermi level is the upper limit of the electron occupied states in a metal at the absolute 0 K. When a bias voltage is applied between the tip and the sample, a tunneling current can occur. The tunneling current I can be derived from the form:

$$I \approx V \rho_s(z=0, E_F) e^{-1.025\sqrt{\Phi W}}, \quad (2.7)$$

where V is the bias voltage, $\rho_s(z=0, E_F)$ is the local density of states, and W is the vacuum width[1]. For a typical value of work function $\Phi = 4$ eV, Eq.(2.7) gives the current decaying factor of about $e^2 \approx 7.4$ per Å.

2.2 Piezoelectric effect

About 120 years ago (1880), Pierre Curie and Jacques Curie discovered the piezoelectric effect. The experiment is shown in Fig. 2.3. A long and thin quartz plate was sandwiched between two tin foils, and an electrometer was connected to the foils. When a weight was applied to generate vertical extension, an electric voltage was detected by the electrometer. They also found that the crystals of tourmaline, topaz, cane sugar, and Rochelle salt can generate electric voltage by mechanical stressing.

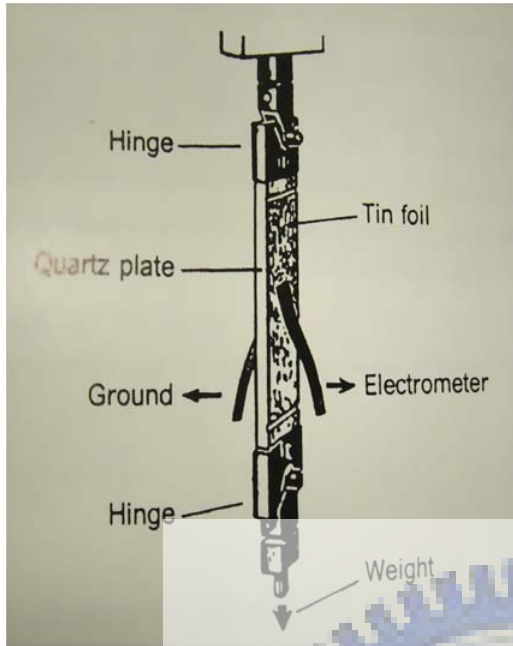


Fig. 2.3. The Curie's experiment. [1]

Besides, an inverse piezoelectric property was mathematically deduced from fundamental thermodynamic principles by Lippmann in 1881 [1]. The Curie brothers immediately confirmed the existence of the "inverse piezoelectric effect," and went on to obtain their quantitative results and material parameters of deformations in the piezoelectric crystals. The experiment designed by Curie brothers is shown in Fig.2.4.

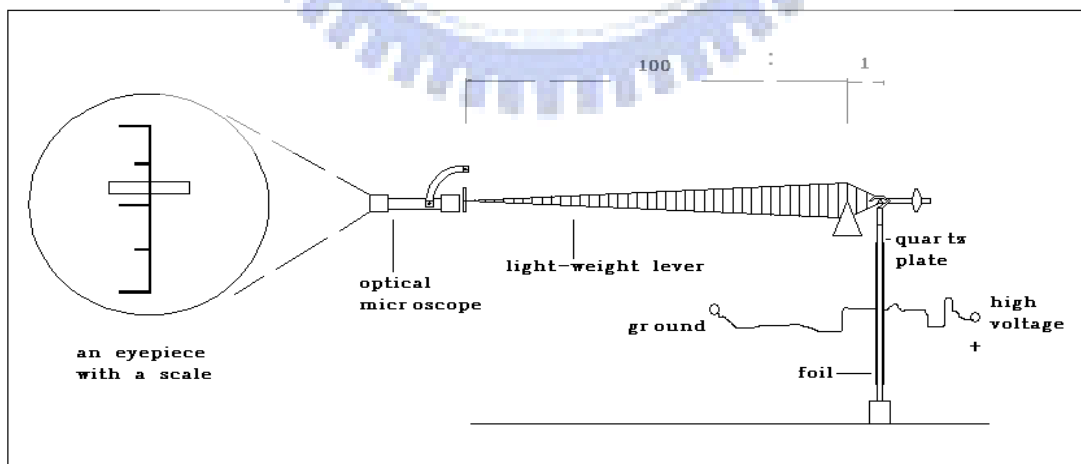


Fig. 2.4. The experiment of the inverse piezoelectric effect. [1]

In the experimental configurations, a thin and long quartz plate was sandwiched

between two conducting tin foils. By applying a high voltage to the tin foils, a deformation of the quartz, either elongation or contraction in according to the polarity of the applied voltage, occurred. To measure the tiny deformation, a lever with an arm of about 1:100 was used to magnify the displacement. An optical microscope was also adopted to reach a much smaller displacement measurement, so the tiny displacement of about hundreds of nanometers could be measured by an eyepiece with a scale.

For describing the piezoelectric effect, some material parameters must be used and they are described as follows.

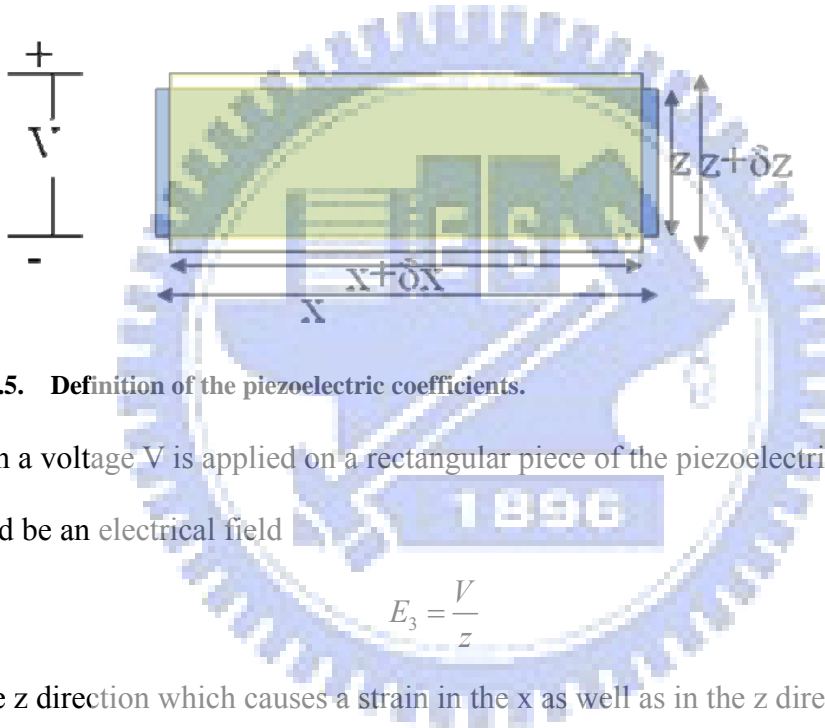


Fig. 2.5. Definition of the piezoelectric coefficients.

When a voltage V is applied on a rectangular piece of the piezoelectric material, there would be an electrical field

$$E_3 = \frac{V}{z} \quad (2.8)$$

in the z direction which causes a strain in the x as well as in the z directions. The xx component of the strain is

$$S_1 \equiv \frac{\delta x}{x}, \quad (2.9)$$

and the zz component is

$$S_3 \equiv \frac{\delta z}{z}. \quad (2.10)$$

Then the piezoelectric coefficients are defined as

$$d_{31} \equiv \frac{S_1}{E_3} \quad \text{and} \quad d_{33} \equiv \frac{S_3}{E_3}. \quad (2.11) \text{ and } (2.12)$$

The piezoelectric coefficients have dimension of meters/volt in SI unit. But their

values are always so small that the $\text{Å}/V$ is more suitable for their application in building STM.

Various kinds of lead zirconate titanate (PZT) ceramics are used as piezoelectric materials in building STM. “The PZT ceramics are made by heating a mixture of PbZrO_3 and PbTiO_3 together with a small amount of additives at $\sim 1350^\circ\text{C}$ under strictly controlled conditions” [1]. The table below shows the important properties of PZT ceramics commonly used in building STM.

Item	Unit	PZT-4D	PZT-5A	PZT-7D	PZT-8
d_{31}	$\text{Å}/V$	-1.35	-2.74	-1.00	-0.97
d_{33}	$\text{Å}/V$	3.15	5.93	2.25	2.25
Y	$10^{10} N/m^2$	7.5	6.1	9.2	8.7
ρ	g/cm^3	7.6	7.5	7.6	7.6
c	km/sec	3.3	2.8	2.9	3.4
T_c	$^\circ\text{C}$	320	195	325	300
E_d	kV/cm	>10	4	>10	>15
Q_M	-	600	65	500	1000
k_p	-	-.60	-.65	-.48	-.51
Aging	$k_p/\text{time decade}$	-1.7%	-0.2%	-0.006%	-2.3%

Table 1.1 The important properties of some PZT ceramics. [1]

The first application of the piezoelectric effect was sonar for detectors of submarines during World War I. With the advance of the technology, it has been widely used as sensors, actuators, loudspeakers, and also employed as important elements in watches and clocks industry.

2.3 Scanning tunneling microscope

The scanning tunneling microscope was invented by Binnig and Rohrer in 1980s, and

they were soon awarded the Nobel Prize of Physics in 1986. It consists of three major parts of mechanical fabrications, electronics, and computer control.

1. Mechanical part: a probe tip, the scanner, the sample, coarse positioner, vibration isolation, instrument frame, etc.
2. Electronics part: the current amplifier, the feedback control, A/D and D/A converter, etc.
3. Computer program: computer control, image process and analysis, etc.

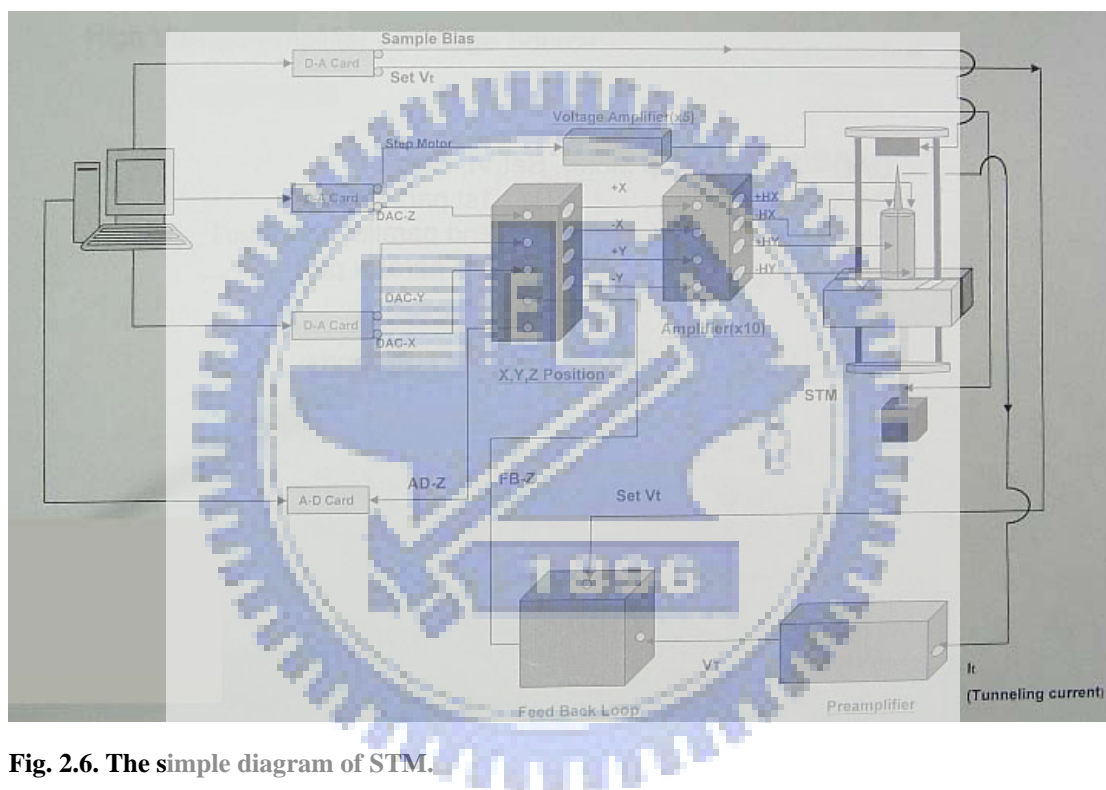


Fig. 2.6. The simple diagram of STM.

The coarse positioner is a so-called stepper. Its mission is to bring the tip to the sample as close as within 1 nm. With a bias voltage applied between the tip and the sample, a tunneling current occurs. The tunneling current in STM is too small, typically from 0.01 to 50 nA, to be free from external disturbance. Thus, the current amplifier, which amplifies the small tunneling current and converts it into a voltage, is essential to the STM instrument. The voltage is compared with a reference voltage value, and the difference is then fed back to drive the scanner.

The **scanner** is a piezoelectric driver which controls the x, y, and z-axis motion. The tube type scanner (see Fig. 2.7) is commonly used in STM instrument, today. It is a PZT tube with metal thin films deposited on both inner and outer surfaces as electrodes. The outer electrode is sectioned into four parts as four quadrants. The inner electrode is connected to the z voltage of the electronic controller. If we apply $+V_x$ and $-V_x$ voltages on two of the opposite outer electrode parts, one would be elongated while the other would be contracted. By this way we can make the tube bending in the x-direction (see Fig. 2.8) as well as in the y-direction.

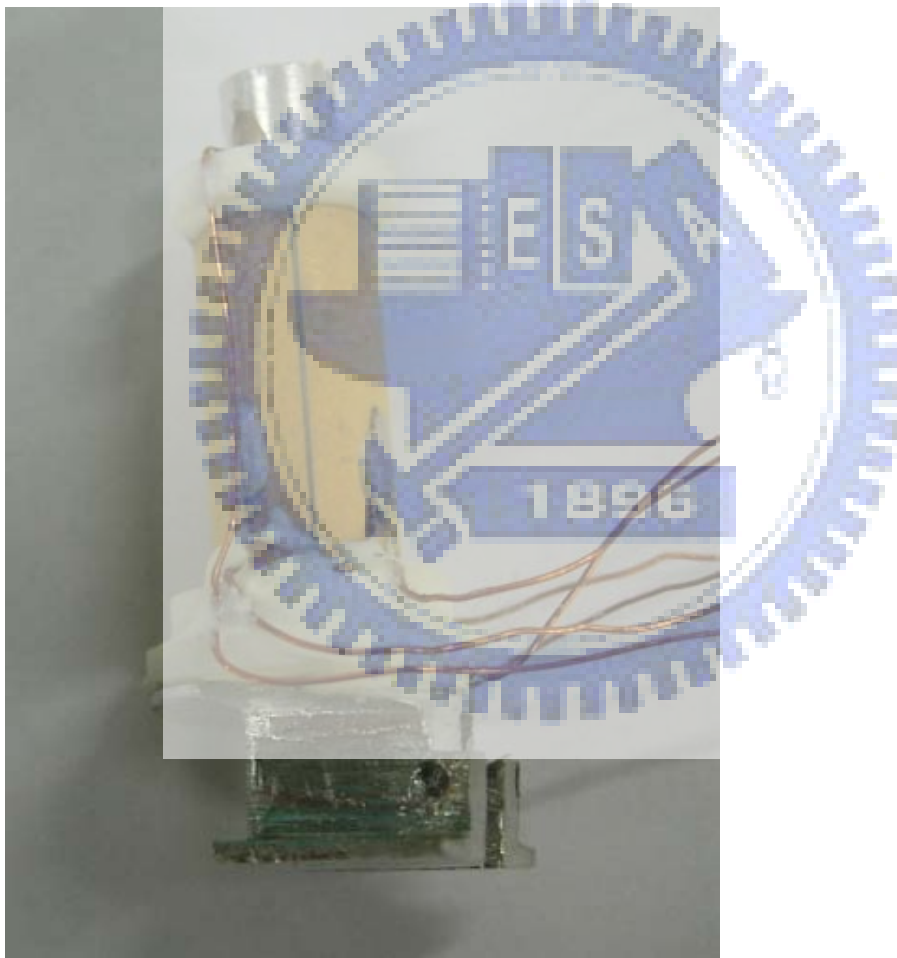


Fig.2.7. The tube scanner. [3]

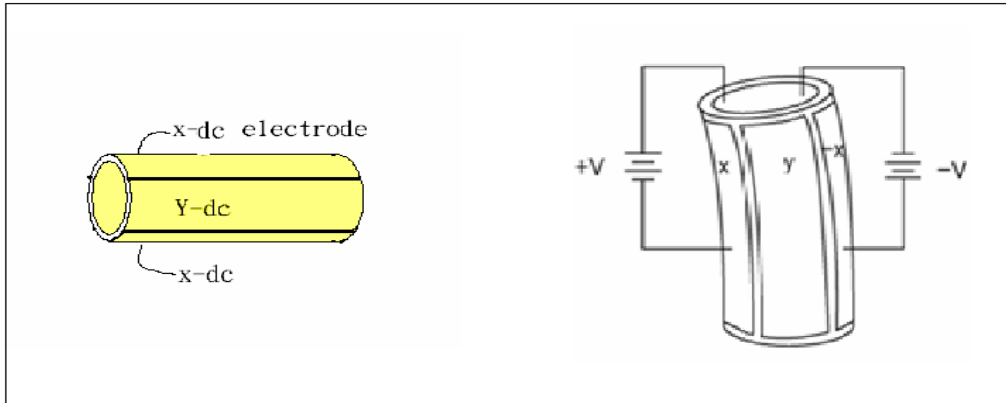


Fig.2.8 The tube bends by applying a voltage.[3]

If all the four outer electrode parts are elongated or contracted by applying the same voltage, the scanner move in the z-direction.

The two-dimensional image (see Fig. 2.9) can be obtained by using the scanner to move the tip going forward and backward in x- or y- directions on the sample and taking the height value of every pixel.

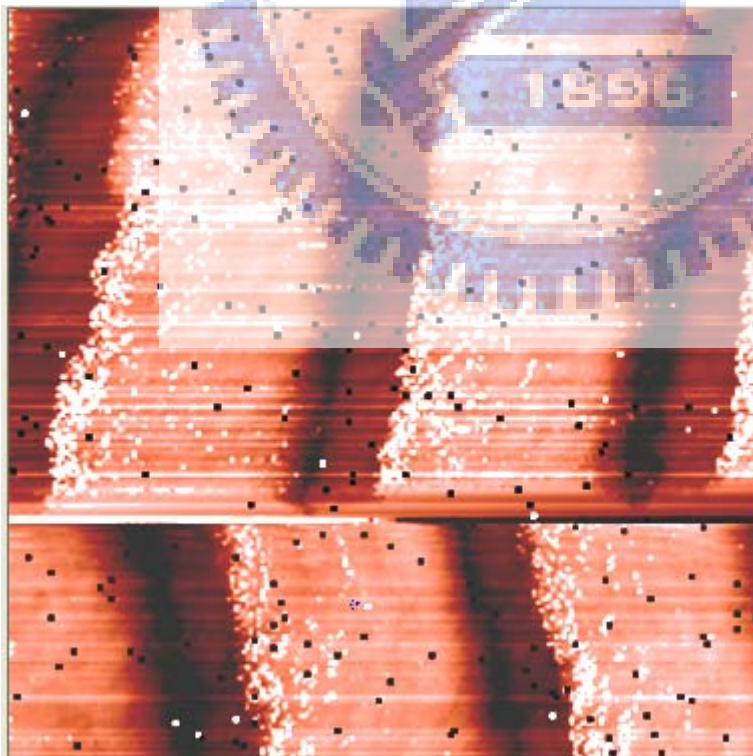


Fig. 2.9. The image of scanning a DVD master. We can see it scans line by line. (The image of this

picture is taken from a continuous scanning mode. It presents us a somehow different topography from the previous scan. This may be due to the thermal perturbation.)

The method of taking images can be classified into two main mode:

1. Constant current mode

The constant current mode is to set a reference tunneling current value for the feedback signal. Because the tunneling current is very sensitive to the distance between the tip and the sample, the set tunneling current would fix the distance between the tip and the sample. When the tip is scanning on the sample surface, the height of the tip would be adjusted to the topography of the sample.(Fig. 2.10.) Thus taking the image of the tip's height would reflect the topography of the sample. The advantage of this method is that it can measure irregular surfaces with high precision; the disadvantage is that the scan rate is so slow owing to the need of feedback control that the scan is easily interrupted by low frequency noise.

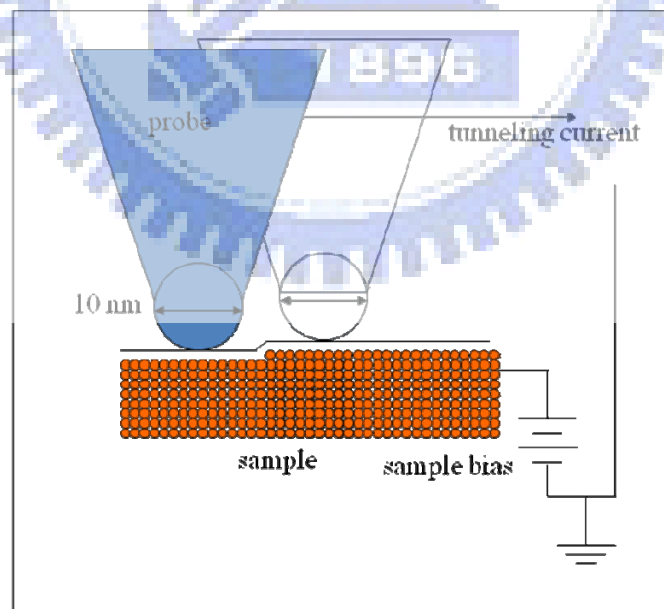


Fig. 2.10. The constant current mode. The distance between the tip and the sample is fixed at a set value.

2. Constant height mode

The constant height mode is to take image directly from the value of tunneling current at each location. When the tip is scanning at a set height, the tunneling current would vary depending on topography of the sample(Fig.2.11). The advantage of this method is that it scans fast so it can capture some dynamics properties of surface; the disadvantage is that it provides useful information only for relatively smooth surfaces. If the surface is too irregularity, the tip or the sample would easily get destruction.

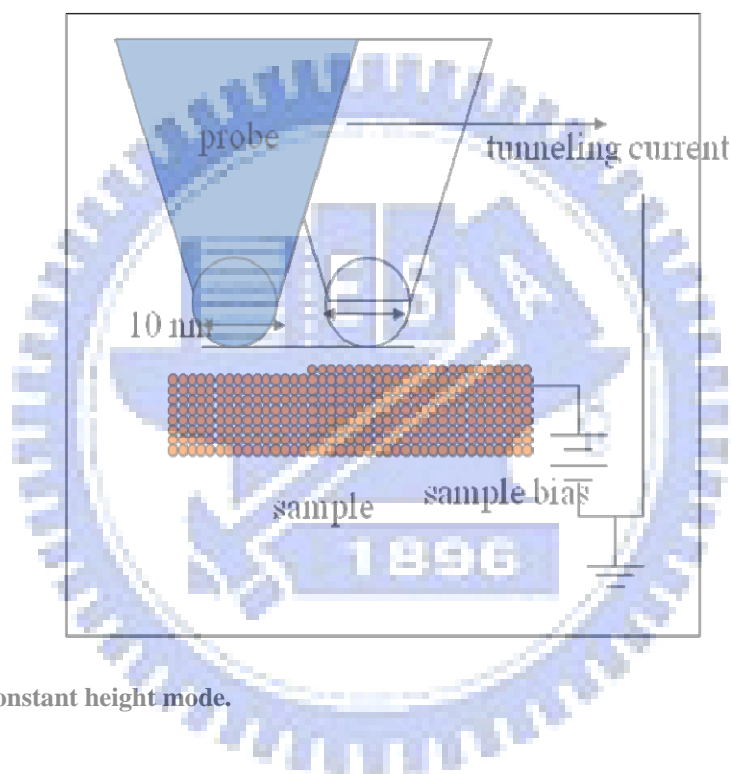


Fig.2.11. The constant height mode.

Strictly speaking, the image of STM reflects not only the topography of the sample but also the electric properties of the sample. More accurately, the tunneling current corresponds to the electronic density of states at the surface. If the sample is doped some distinct conductivity material or the sample has oxidized, we must especially check what it really is when we are interested in mapping topography. The other elements of STM will be mention in detail in the forward experiment chapters.

Chapter 3 Experiments

3.1 The mechanical part

3.1.1 Disk scanner

We use the audio transducer as the disk scanner. It consist of piezo-ceramics glued onto a brass plate (see Fig. 3.1.) and is one of the most common piezoelectric devices which is often used for the small sound generator, speaker, buzzer.



Fig. 3.1 The audio transducer. It is easily obtained in most electrical material shops.

By applying a voltage between the brass plate and the metal electrode, the disk bows up or down.(Fig. 3.2. and Fig. 3.3.)

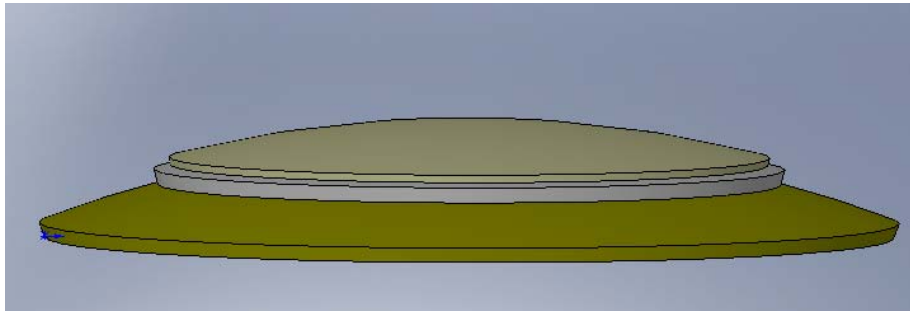


Fig. 3.2. The disk bows up.



Fig 3.3. The disk bows down.

In order to get scanner motion in x-y-z axis, we divide the electrode into four quadrants.(Fig.3.4.) And we add a base at the center. Also we image a pointer set at the center base for explanation.

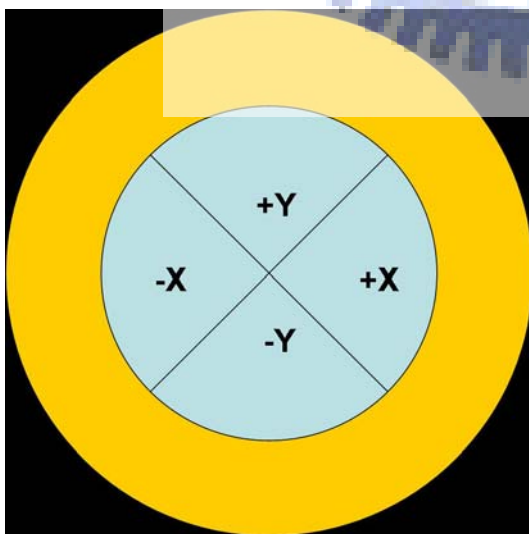


Fig. 3.4. The electrode is divided into four quadrants.

As the voltage we supply to an electrode is different from the opposing one, there would be an angle change of the pointer, as the figures shown below.

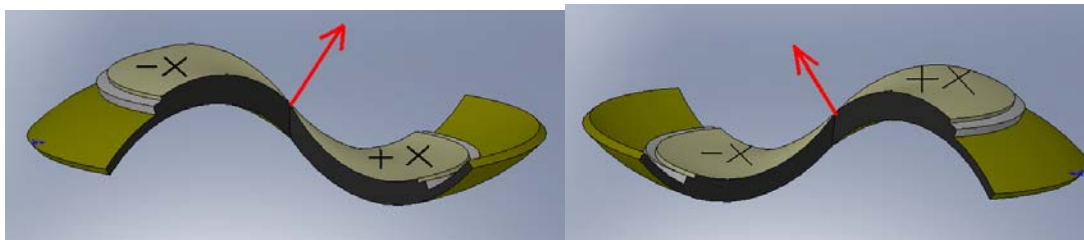


Fig. 3.5. The X -scanning. The Y -scanning is in the same way. Of course these figures are exaggerative. Since the angle change is so small that the scanner can scan with good linearity.

Similarly the Z-axis motion can be achieved by applying the same amount voltage to all four quadrants.

After dividing the electrode into four quadrants, we glue an isolation ceramic pipe to the center with AB glue. The isolation ceramic pipe is used as the base of tip holder (Fig.3.6.) .Then four conducting wires are individually contacted to the four electrodes with silver paste gluing them. To ensure stably contacting, we may weld the wood's metal, a kind of low melting point solder, at the contact points. To finish up the scanner we glue the disk part to the scanner holder (Fig.3.7.) with a round hole in the center with silver paste. This can let the brass plate of the disk electrically contact to the grounded STM frame. The Scanner is now complete.(Fig.3.8.)

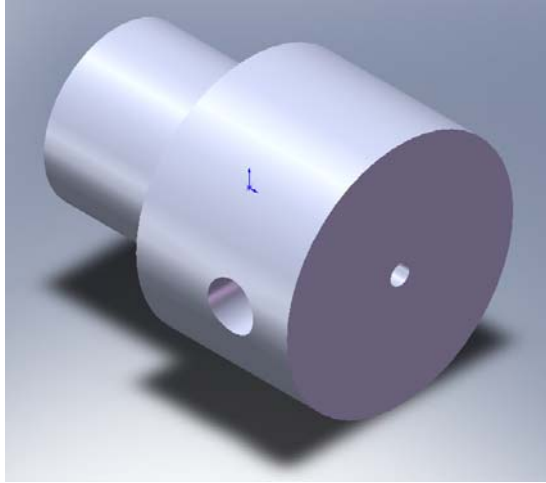


Fig.3.6. The tip holder made by red bronze.



Fig.3.7. The scanner holder made by aluminum alloy.

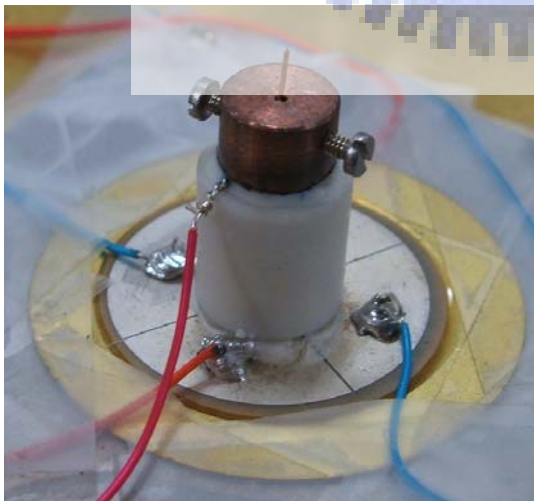


Fig.3.8. The disk scanner with a tip locked at the tip holder.

3.1.2 Sample stage

We apply the bias voltage to the sample, so the sample holder must be a conductivity material. But the sample holder should be isolated from the grounded STM frame. So we choose a quartz piece to do the job because the quartz has good rigidity and low thermal expansion coefficient. The sample holder is a square piece of stainless steel which can be attracted to a magnet. The magnet we use is NdFeB, a kind of strong magnets, with metal coating. By gluing it on the quartz piece, the sample holder can be strongly attracted to it. Of course, a conducting wire is connected to the bias voltage output. Then the sample stage is simply completed.



Fig. 3.9. The sample stage.

3.1.3 Tip

The tip is generally made by Au or W wires with 0.3 or 0.5 mm in diameter. They are prepared by electrochemical etching. Besides the gold and tungsten tips, a Pt-Ir wire by mechanically cutting out can also work in STM.

The characteristics and composition of the tip play an important role in the

resolution of the STM. Ideally, the tip needs to have one atom on its apex, but it is too hard to be done. Practically, a tip with an apex radius of less than 50 nm is sharp enough to obtain atomic resolution.

There are three basic requirements for tip preparation: short length, high symmetry, and sharp apex.” *Short length is necessary to decrease mechanical vibrations that will blur the image. High symmetry will yield an electronic wave function symmetric that will yield an undistorted image (the image is the convolution of the electronic wave functions of tip and sample). Finally, a sharp apex will avoid changes of the microtip that is actually responsible for the tunneling current*”.[4]

The method of tip preparation is that tips are etching in a solution of KOH (for tungsten) or HCl (for gold). The steps of tip fabrication are: (Fig.3.10)

1. A tungsten wire (gold wire) is vertically inserted in a solution of 2M KOH (HCl).
2. The cathode is a piece of stainless steel.
3. A positive voltage, 4V to 12V (1V to 2V), is applied to the wire, which is the anode.
4. Etching for about 10 minutes (5 minutes), the neck of the wire fractures by the weight of the inserted part.

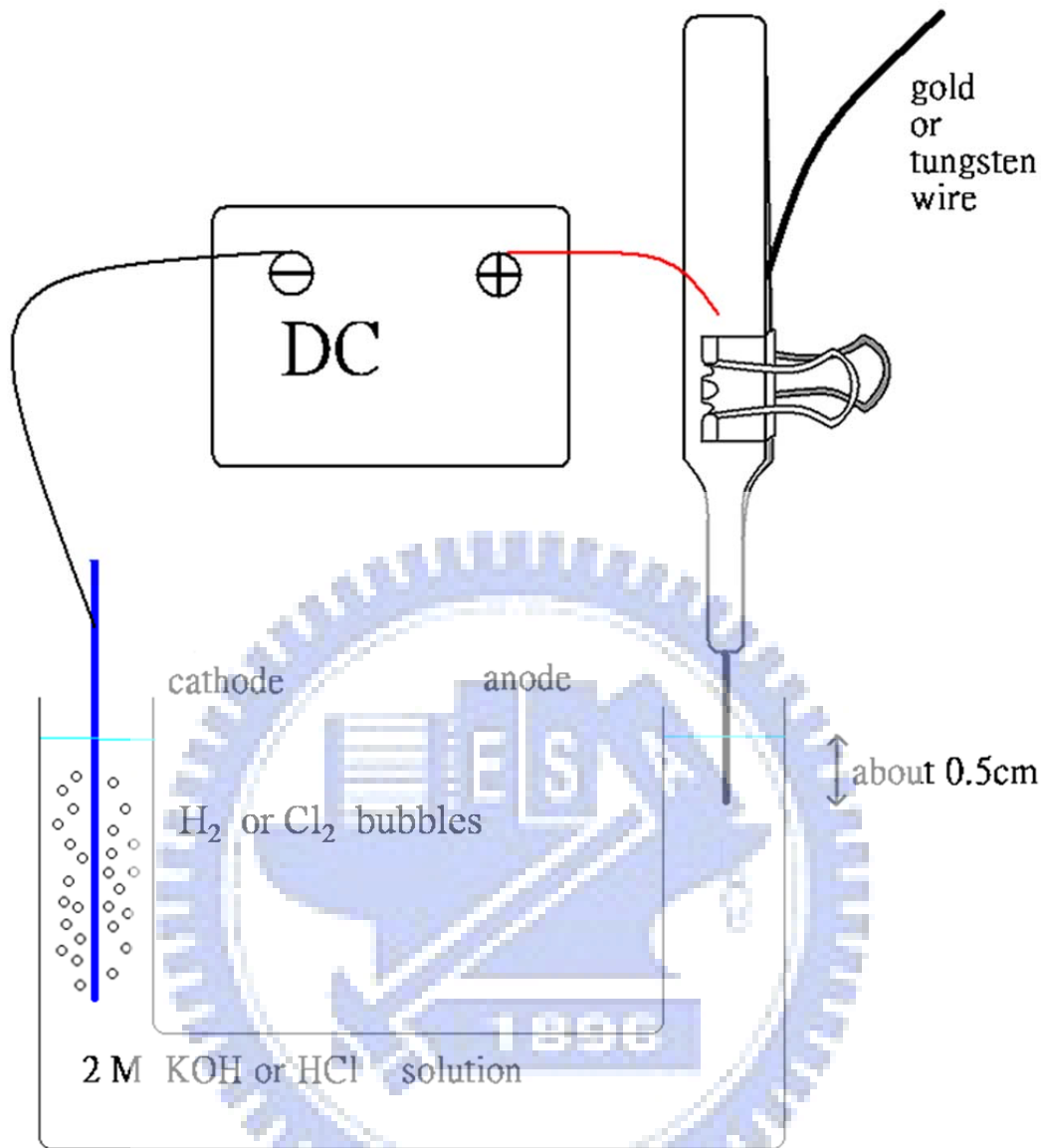


Fig.3.10. Electrochemical etching of tungsten or gold tips. (Drawn by Guo 2007)

During a scan, the tip often undergoes unexpected and spontaneous changes that may influence the look and the resolution of STM images. Since the randomness property of tip condition is unavoidable, we can sharpen the tip by immediately applying a strong electrical field to make atoms of the apex realignment.



Fig. 3.11. The SEM images of a W tip. (Captured by Y. F. Lin.)

3.1.4 Vibration isolation system

“Effective vibration isolation is one of the critical elements in achieving atomic resolution by STM. The typical corrugation amplitude for STM images is about 0.1 \AA . Therefore, the disturbance from external vibration must be reduced to less than 0.01 \AA ”[1]. Maintaining the relative distance between the tip and the sample is also the purpose of vibration isolation. The amplitude of vibration of various frequencies should be minimize. The vibration isolation elements commonly used are springs or vitons (橡皮墊) together with dampers. The resonance frequency of a well designed system is down to 2~3 Hz. A high rigidity of the structure between the tip and the sample can overcome the extremely low frequency vibration.

We construct the vibration isolation system by using suspension springs made by stainless steel with appropriate original length.

3.1.5 The STM frame and the stepper

The design of our STM frame is very simple in geometry appearance for easily manufacturing, and the most parts of frame are consists of aluminum alloy for light weight. The disk scanner holder is put on the lower plate of frame, and the sample stage is glued to the upper plate of it. In order to receive a high rigidity between the sample and the tip, we select a heavier material of brass as the upper plate with three micrometrical screws as crutches, which indent on the lower plate by gravity. The three micrometrical screws play the rules of **stepper**. The two near sample screws function as coarse step while the far one functions as fine-step by the **lever principle**. The lever's arm is about 1:100 and the screw is an 1/4"-80 fine adjustment screw. When we operate the STM practically, we can let the tip do a nanometer move of tunneling current scale by rotating the screws by hands. One of side plates is

preserved to do the connection between the frame and the electronics box.

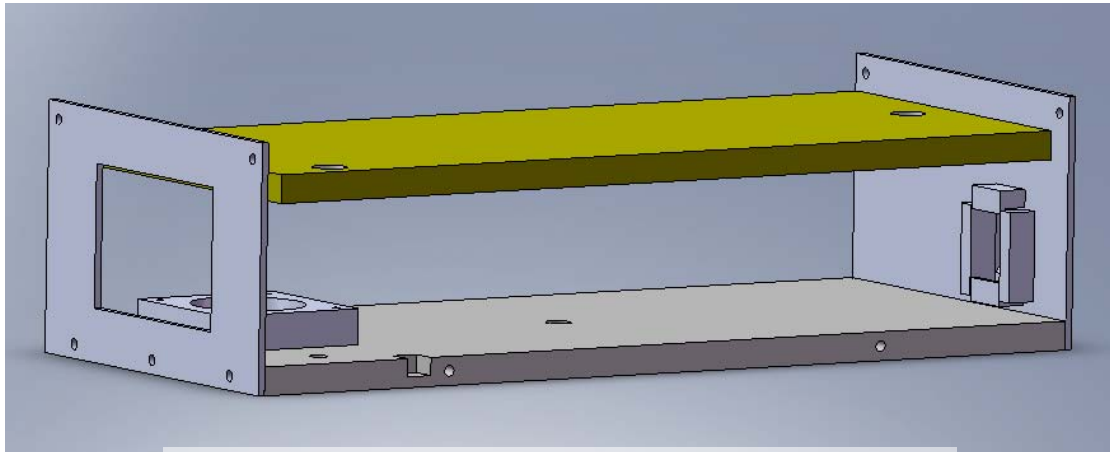


Fig.3.12 The STM frame.(The disk scanner, sample stage, screws, springs, and connection wires are omitted.)



Fig.3.13 The 1/4"-80 fine adjustment screw.

3.2 Electronic part

The method of taking STM images we use is **constant current mode**. So we must design an electric circuit to detect the height of tip describing the topography of sample. The height of tip is reflected in Z-axis motion of the disk scanner. Also we must design a feedback system to fix the tunneling current at a desired value.

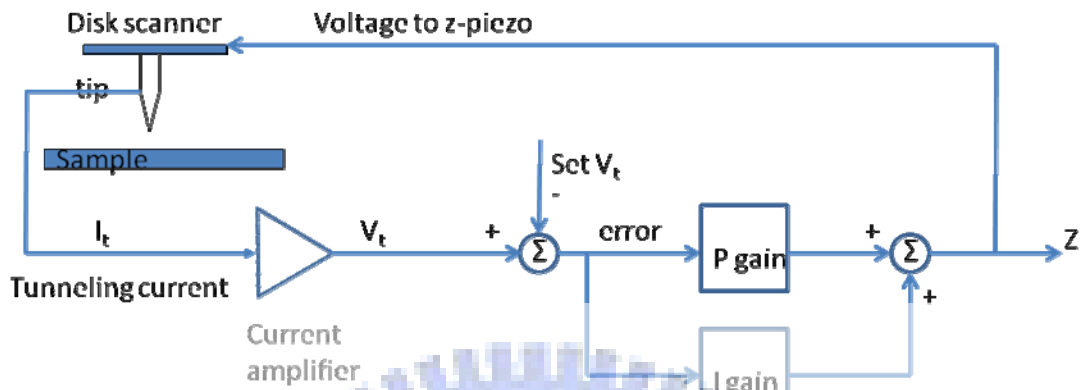


Fig.3.14. The conceptual diagram of Z-axis feedback system in STM.

Combining the computer interface and the X-Y-Z position, the electronic part is complete.

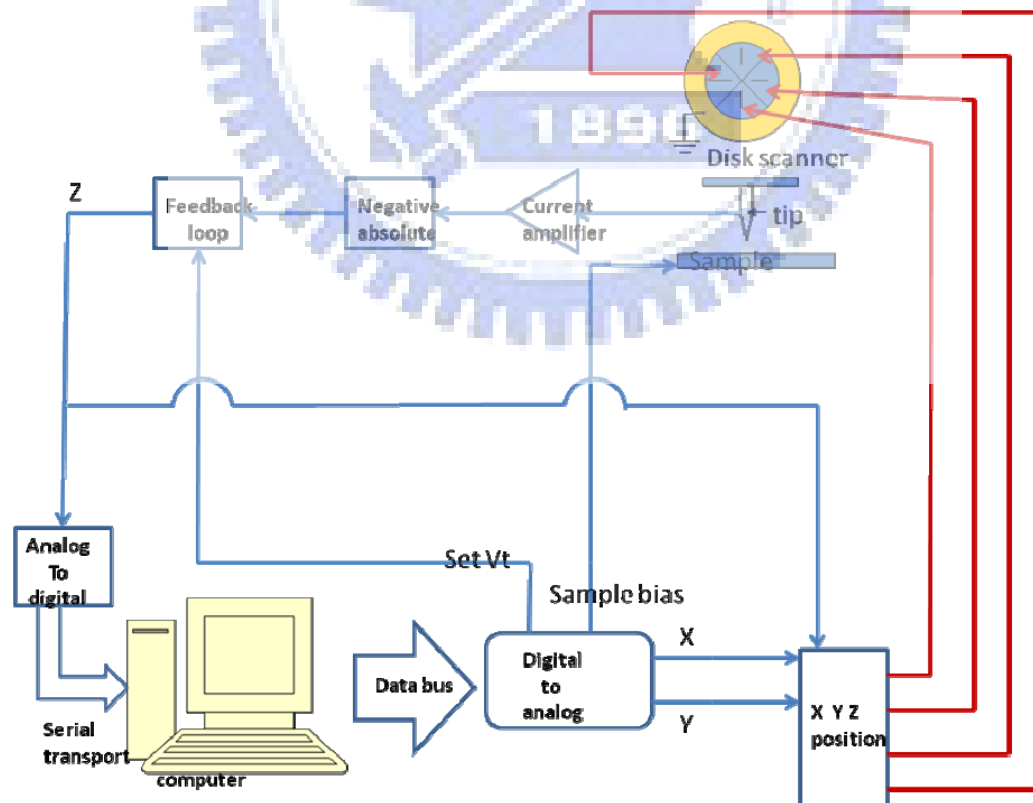


Fig.3.15. The whole electronic elements of our STM.

3.2.1 Current amplifier

A current amplifier is necessary to detect the very low tunneling current. The typical current to voltage amplifier is shown in Fig.3.16 .

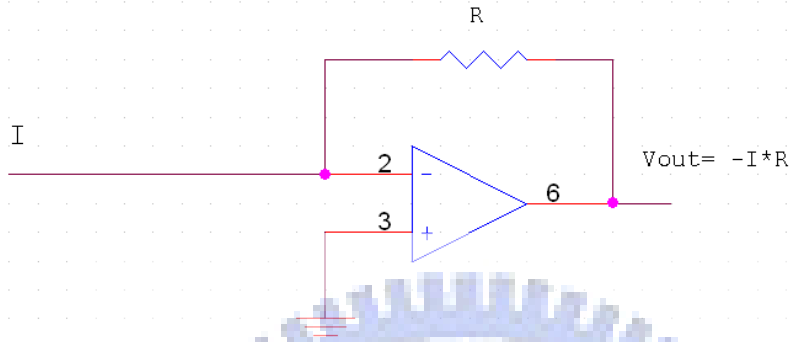


Fig.3.16. The current to voltage amplifier. The feedback resistor R dominates the gain.

A typical value of the feedback resistor used in STM is $10^8 \Omega$. There are also some inevitable parasitic capacitances in the amplifier circuit. Those parasitic capacitors, the thermal noise of the feedback resistor, and the characteristics of the op-amp can affect the performance of the current amplifier.

Preamplifier

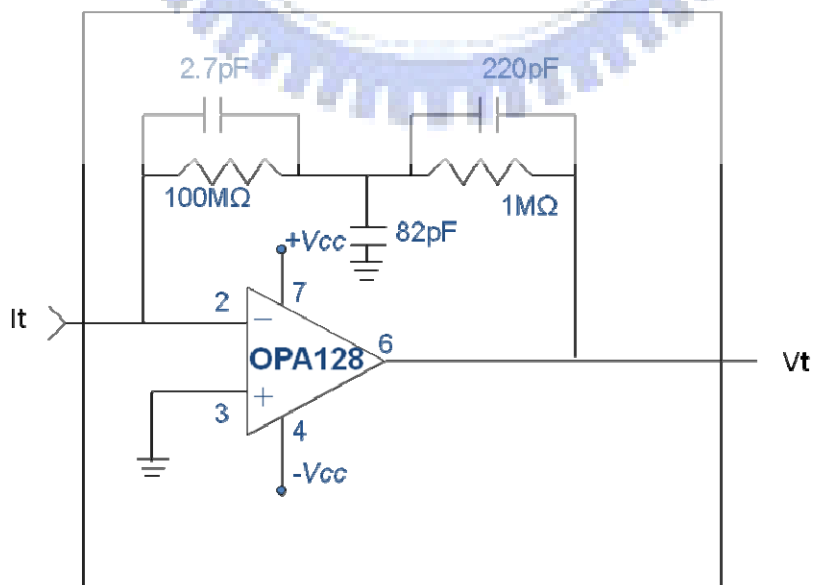


Fig.3.17. The current amplifier we use. The noise we tested is below 10 mV.

3.2.2 Feedback loop

We constitute a negative feedback: If the tunneling current is smaller than the set current, the voltage applied to the z-piezo tends to approach the tip to the sample surface, and vice versa.

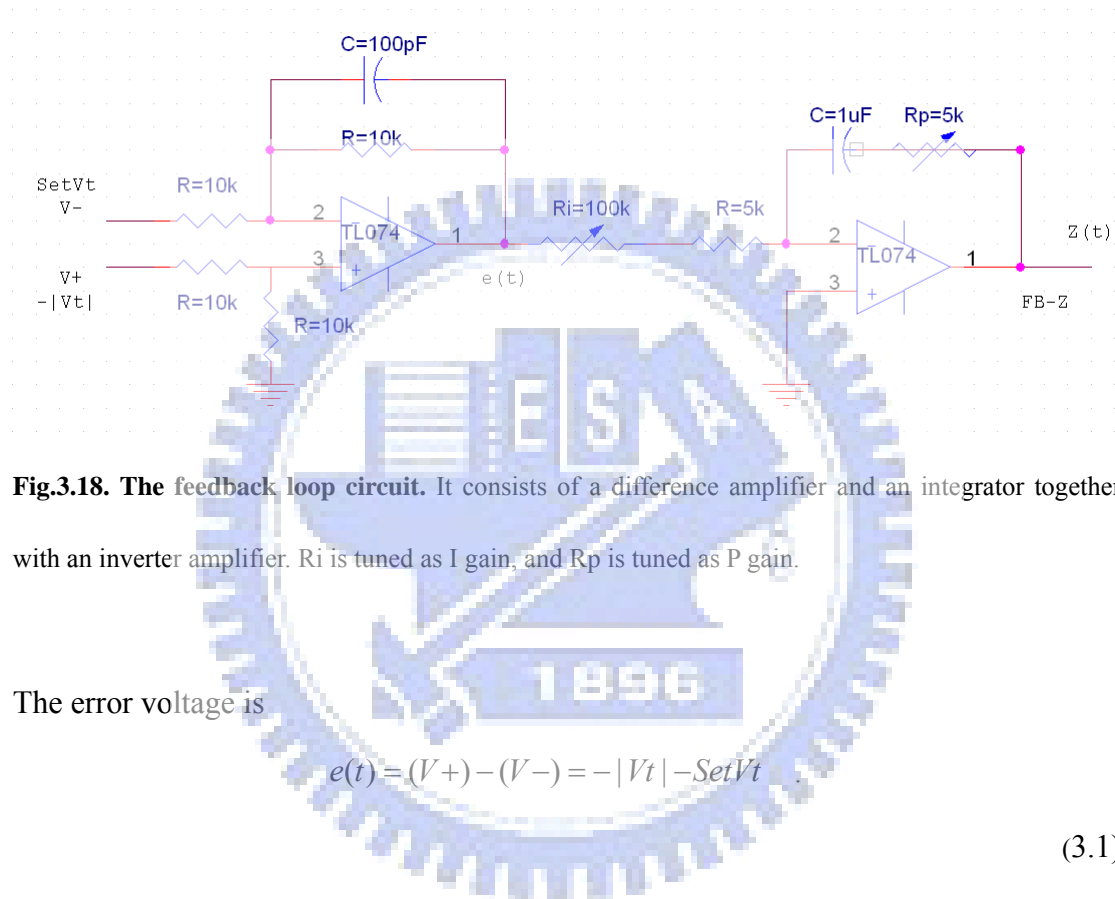


Fig.3.18. The feedback loop circuit. It consists of a difference amplifier and an integrator together with an inverter amplifier. R_i is tuned as I gain, and R_p is tuned as P gain.

The error voltage is

$$e(t) = (V+) - (V-) = -|Vt| - SetVt \quad (3.1)$$

And the output of the feedback loop $z(t)$ is

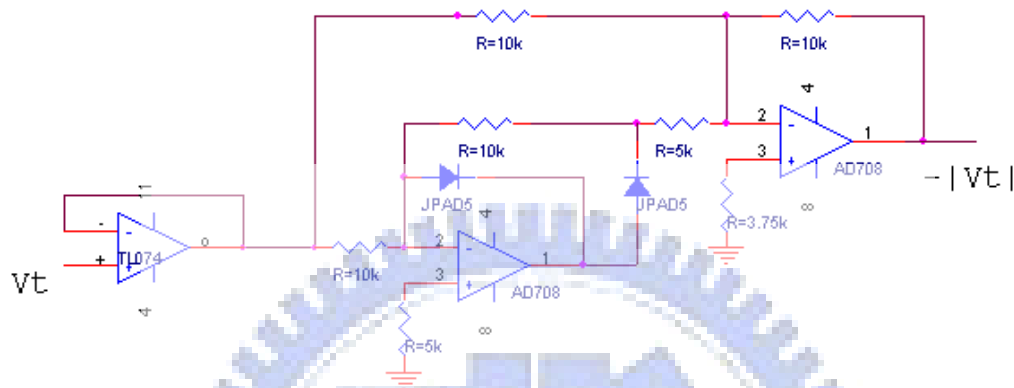
$$z(t) = \frac{-1}{(R_i + 5k)} \int_{t_0}^t e(t') dt' - \frac{R_p}{(R_i + 5k)} e(t) + z(t_0) \quad (3.2)$$

The above shows we use the PI-controller. The D-controller is generally unused because a differentiator amplifies high frequency noise.

3.2.3 Negative absolute circuit

The sample bias we apply may be positive or negative. So the tunneling current may

be from sample to tip or from tip to sample. Then the V_t , output of the current amplifier, may be negative or positive. A trouble will happen in feedback loop if we directly compare V_t with $SetV_t$. So we design a **negative absolute circuit** to ensure the voltage compared with $SetV_t$ is negative.



(Negative absolute value circuit)

Fig.3.19. The negative absolute circuit. It is often used as the full-wave-filter circuit.

3.2.4 X-Y-Z position

We apply periodic ramp voltages to the X -and Y- piezo to make the scanner do the X-Y scanning. And the Z-piezo voltage must be added to the ramp voltages to adjust the tip's height at every X-Y location. So we construct a circuit which consists of some inverter amplifier to do the job. Since the disk scanner can work by just applying low voltage to it, the high voltage amplifier is not necessary.

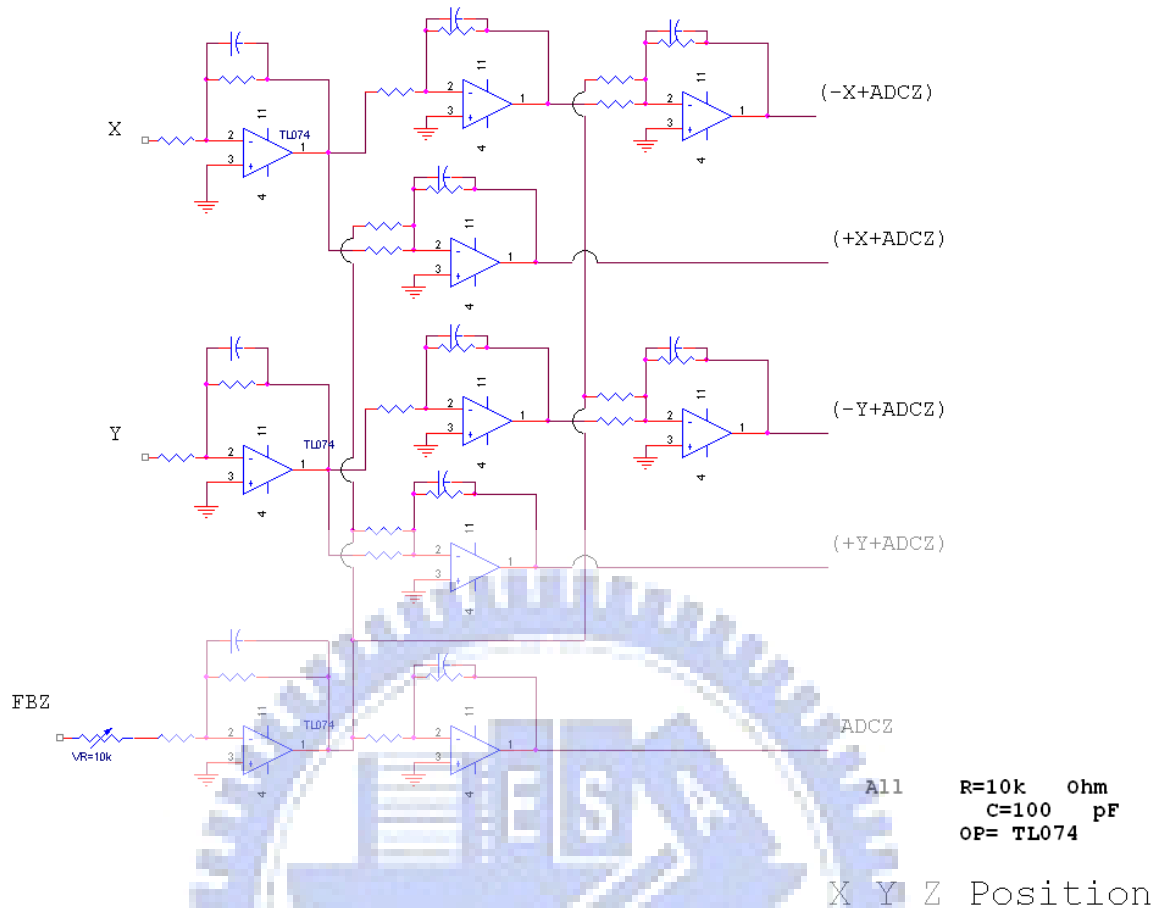


Fig.3.20. X Y Z position. The saturation of op-amp must be still considered when we operate the STM.

3.2.5 Digital to analog circuit

Computer control has been an essential part of STM ever since the beginning. Most of the laboratory STMs and commercial STMs use software and D/A converters to generate scan voltages. We also give the sample bias to the sample and the SetVt to the feedback loop from D/A converters. The D/A converter we use has a full range of -10 V ~ +10 V, with 16-bit accuracy. Each step is $20V/2^{16}=0.000305$ V. By using it directly to drive the x,y piezo with the disk scanner's typical piezo constant of

$0.1 \mu\text{m/V}$, each step is 0.305 \AA .

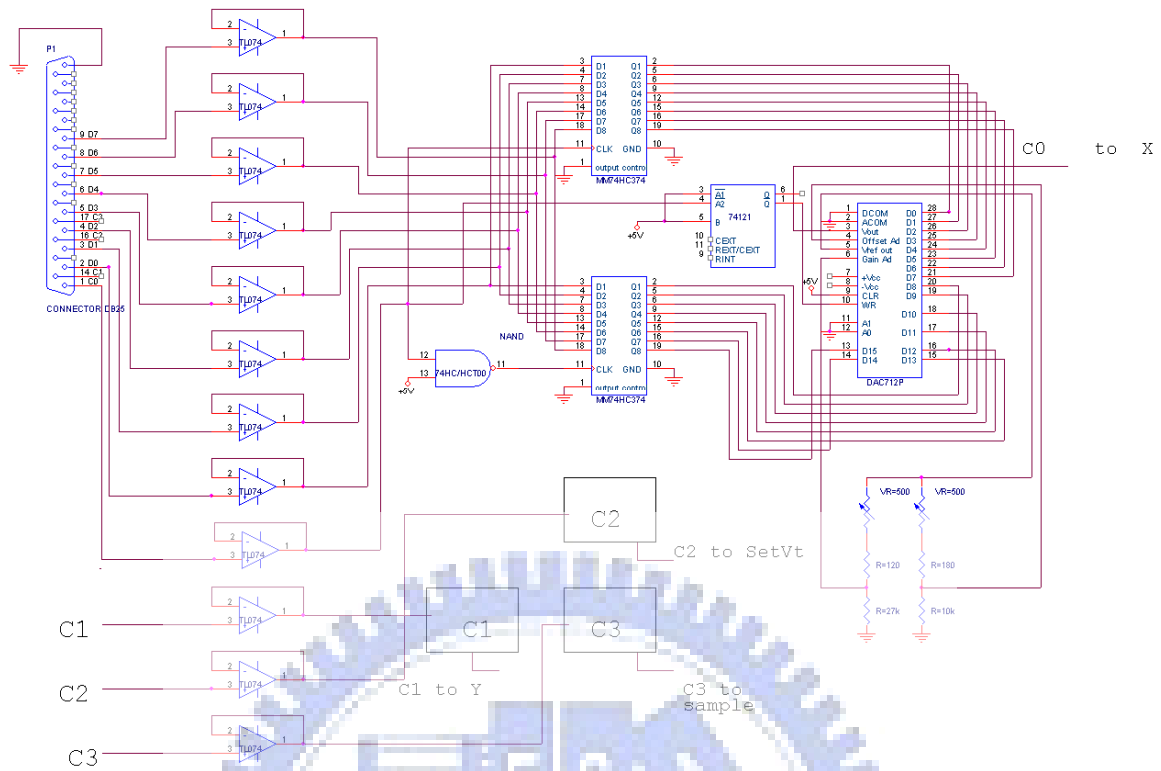


Fig.3.21. The D/A converters.

3.2.6 Analog to digital circuit

The reading of z piezo voltage is taken to the computer with an A/D converter. We use a 16-bit A/D converter with $10 \mu\text{s}$ sampling rate. Each step is also 0.305 mV .

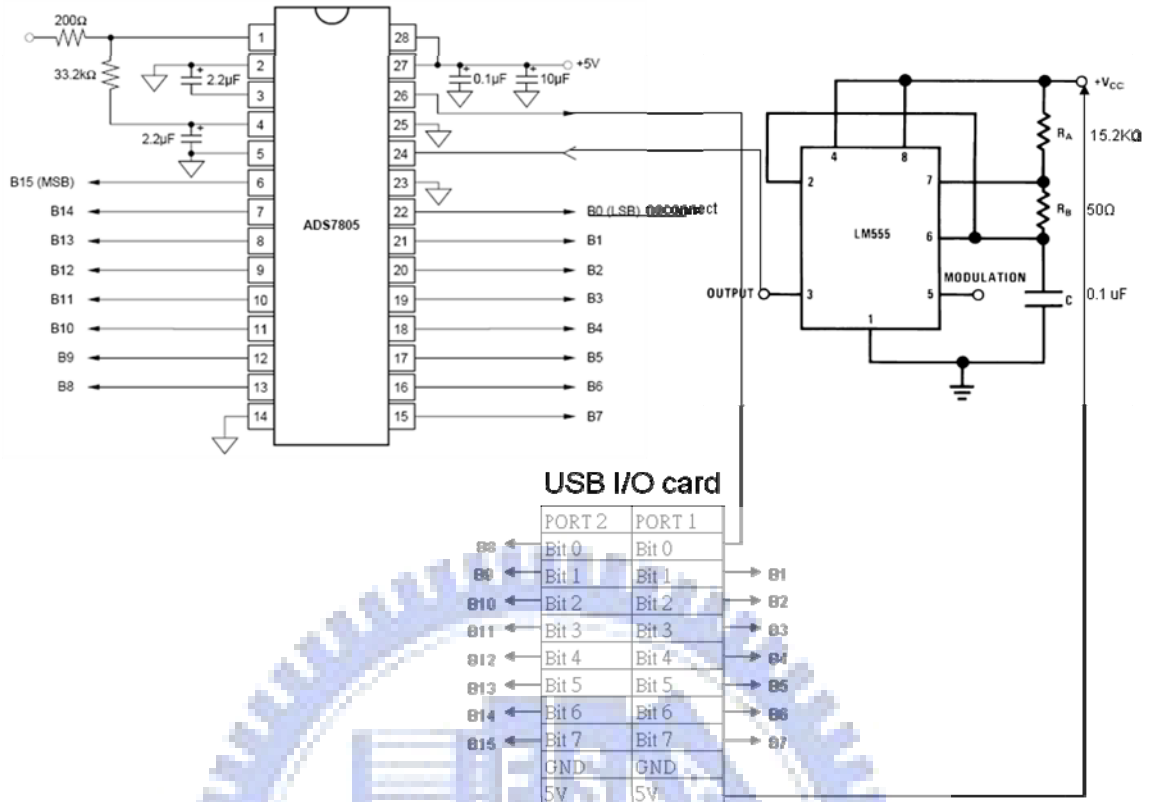


Fig.3.22. The A/D converter.

3.3 Computer part

Control program and analysis software

The STM control program is developed by Prof. Wen-Bin Jian. Most standard parameters of STM are included in this program.

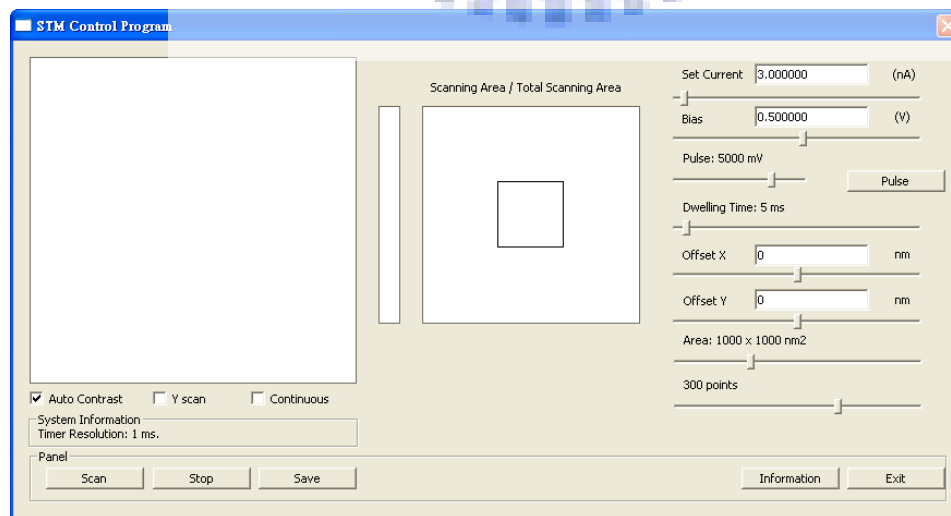


Fig.3.23. The STM control program.

After taking the STM image, the original image should be processed for the convenient of analysis. A Nano-scale Image Processor also developed by Prof. Wen-Bin Jian can do the process and analysis.

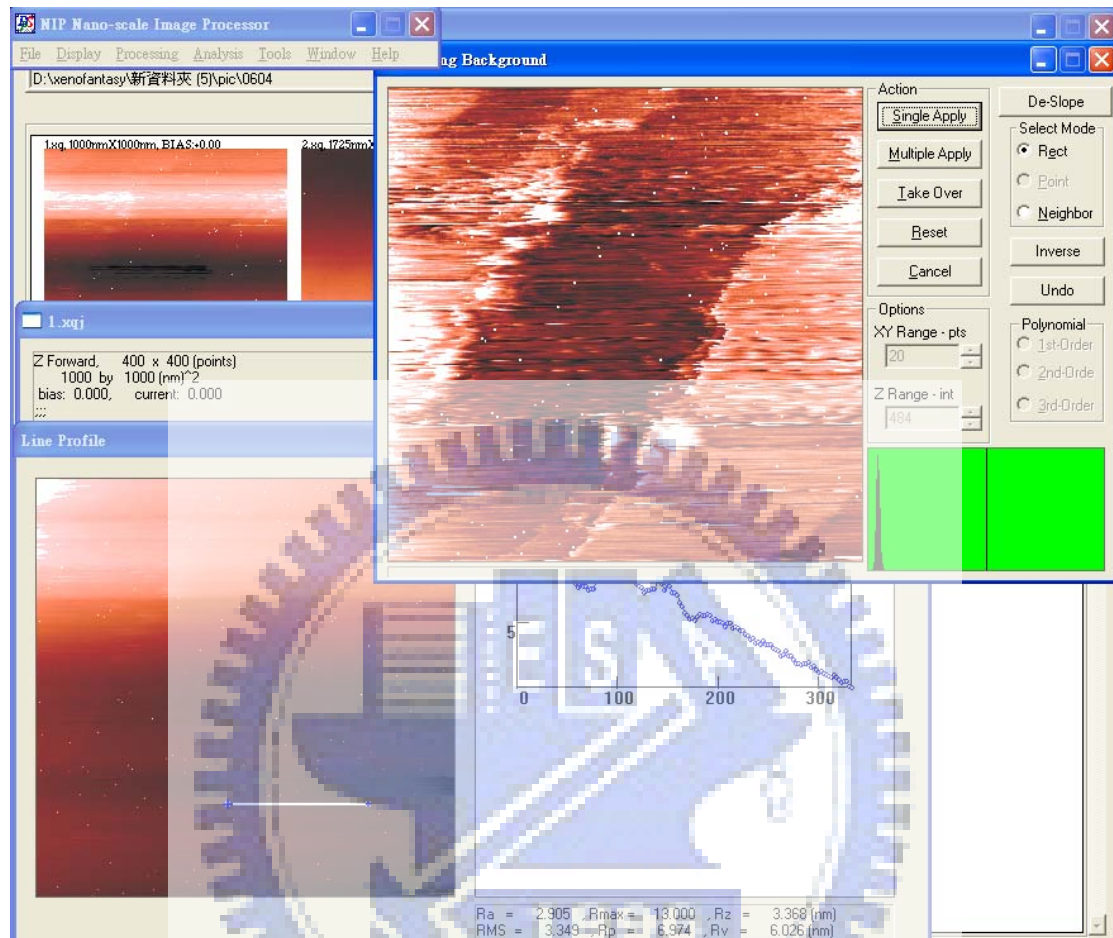


Fig.3.24 The NIP program.

Chapter 4 Results and Discussions

4.1 Spring vibration isolation system

We adapt the simplest method of suspension springs when we design our vibration isolation system. It can be modeled as the one-dimensional system of mass, spring, and damper.[3]

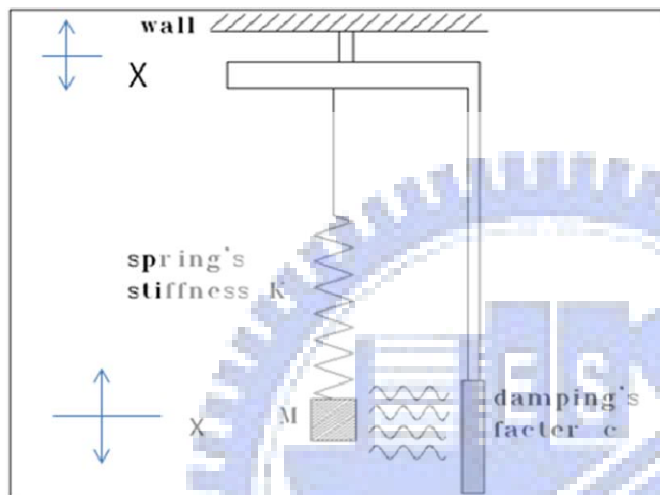


Fig.4.1. The mass, spring, and damper system.

The system is governed by the below differential equation:

$$m\ddot{x} + c\dot{x} + kx = f(t) = c\dot{X} + kX \quad (4.1)$$

$$\omega_0 = \sqrt{\frac{k}{m}} \quad (4.2)$$

$$X(t) = X_0 e^{i\omega t} \text{ for sinusoidal vibration} \quad (4.3)$$

The transfer function is

$$K(\omega) = \left| \frac{x_0}{X_0} \right| = \sqrt{\frac{\omega_0^2 + 4\gamma^2 \omega^2}{(\omega_0^2 - \omega^2)^2 + 4\gamma^2 \omega^2}} \quad (4.4)$$

If the interference frequency is far higher than the nature frequency of the system and the damping is negligible, then the transfer function is:

$$K(\omega) \approx \left(\frac{\omega_0}{\omega} \right)^2 = \left(\frac{f_0}{f} \right)^2 \quad (4.5)$$

So the high frequency excitation can be filtered.

If the excitation frequency is close to the natural frequency of the system, the transfer function would be large.

At the resonance frequency:

$$K(\omega) = \frac{1}{\sqrt{1 + \frac{\omega_0^2}{4\gamma^2}}} \approx \frac{\omega_0}{2\gamma} \quad (4.6)$$

An appropriate damping must be applied to avoid such resonance excitation.

The resonance frequency should be minimized:

$$f_0 = \frac{1}{2\pi} \sqrt{k/m} \quad (4.7)$$

$$\Delta L = \frac{Mg}{k} \quad (4.8)$$

$$\therefore f_0 \approx \frac{5.0}{\sqrt{\Delta L(\text{cm})}} \quad (4.9)$$

So if the elongation length is 25 cm, the resonance frequency is about 1 Hz. For the consideration of filtered frequency and the space use of the system, springs which resonance frequency is about 1Hz to 5 Hz are used.

4.2 Test for designing the feedback loop

Before the design of feedback loop, we must ensure what polarity of the applied voltage would cause the disk scanner to bow up or down. The test steps are:

1. Rotate the micrometrical screws and let the distance between the tip and the

sample be small enough to occur tunneling current.

2. Apply an increasing or decreasing voltage to the disk scanner. Check the tunneling current is increasing or decreasing.

The result of our test is the tip approaches the sample when we apply a decreasing voltage to the disk scanner. This means the disk scanner is bowing up when the decreasing voltage is applied to the electrodes of it. An inverse result occurs when we apply an increasing voltage.

4.3 STM images

Although we approach the tip to the sample carefully, the image we take is hardly soon good. We must always do some tip sharpening patiently to get a good image. We have taken many STM images with good conditions. The graphite is the typical sample when we study **surface science**. We can detect the atomic steps of graphite by the simple STM. This implies that the resolution of our STM is under the scale of one nano meter.

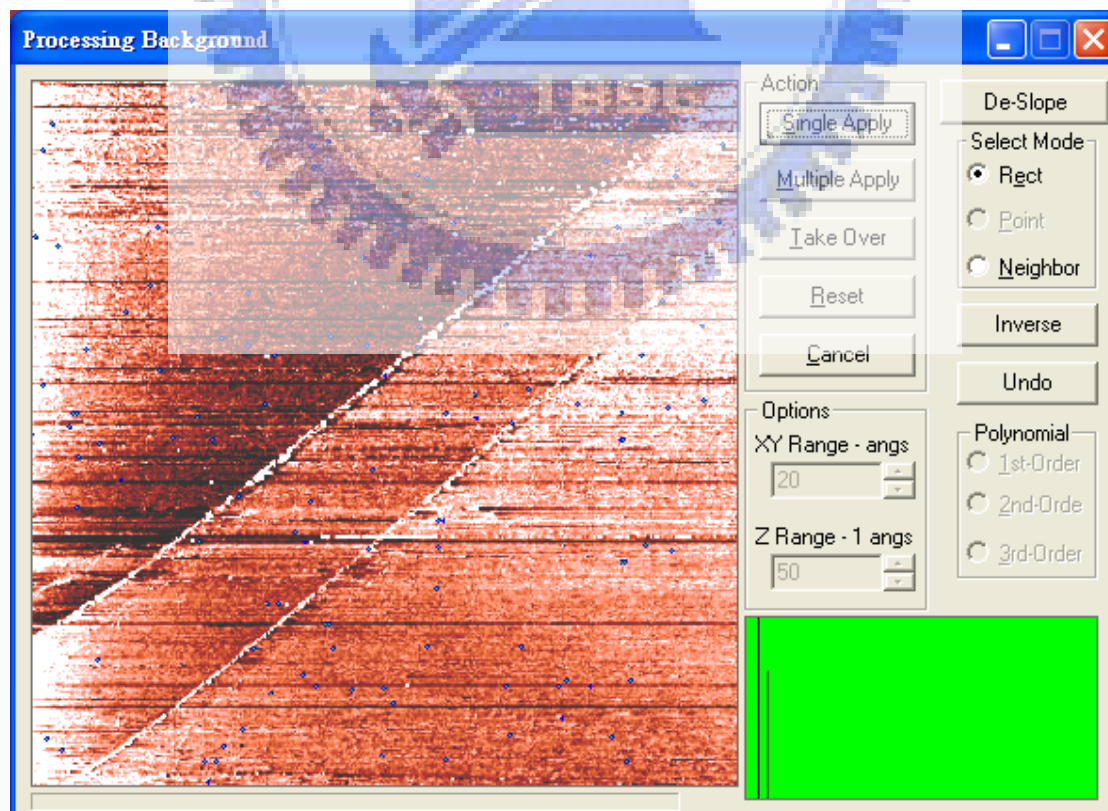


Fig.4.2 The graphite image with 2 steps in the area. (996X996 scan area units)

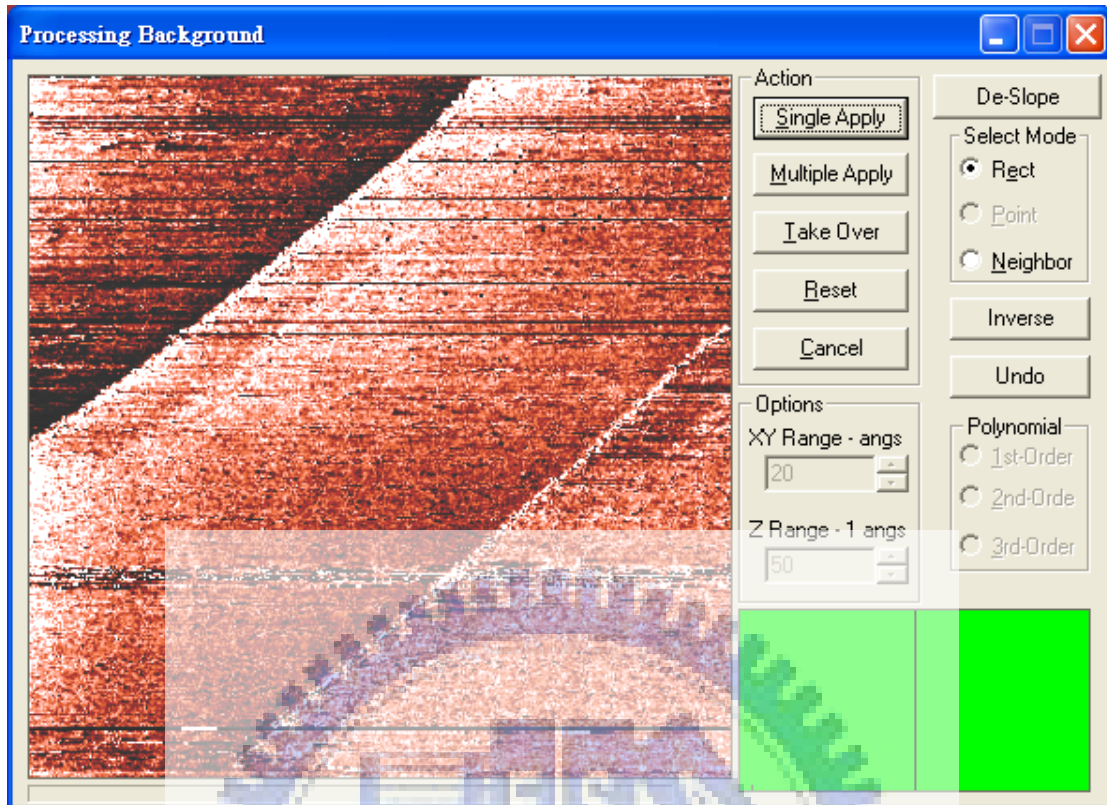


Fig.4.3. The more amplification image of Fig.4.3. (365X365 scan area units)

Fig.4.3 is the amplification image of Fig.4.2. . We can easily find the consistency of the two steps feature of them. So the control parameter of scan area works well.

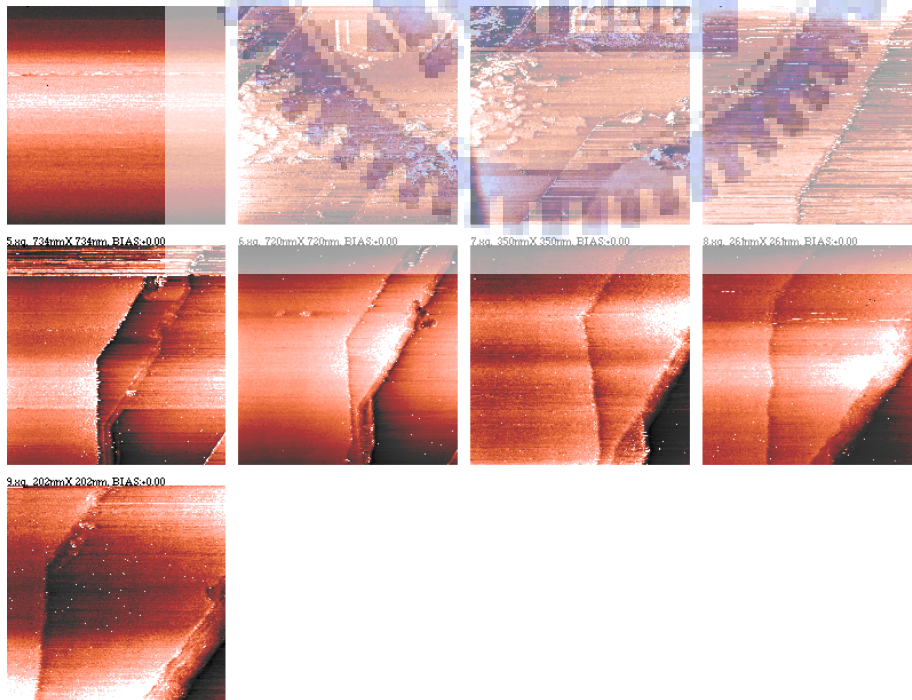


Fig.4.4 A series of scanning images of graphite.

Fig.4.4. shows a series of scanning images of graphite. The last six images were taken in almost the same position of graphite surface with different scan areas. We can find that these images show good consistencies and good reproducible properties. This means our simple STM is very stable and the images are very reliable.

4.4 Calibration

Although we can take good images of graphite surface, we still have no idea of the real scanning area of the disk scanner. So we must prepare a known standard specimen to determine the parameter we want to know. The DVD master with a periodic topography is a good surface for the calibration. To ensure the topography of DVD master, we can also scan the surface by the commercial SPM.



Fig.4.5. The topography of DVD master surface taken by the commercial SPM in our laboratory.

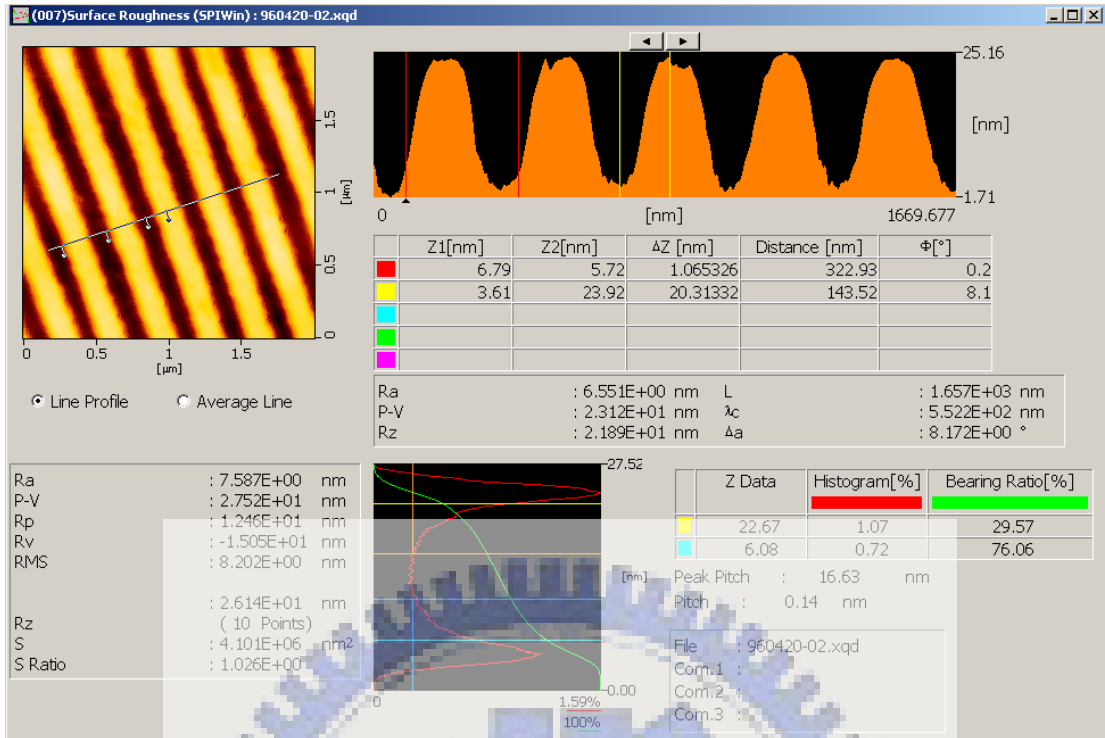


Fig.4.6. The data analysis of Fig.4.5.. It shows the period of the line pad is about 320 nm and the height of it is about 20 nm.

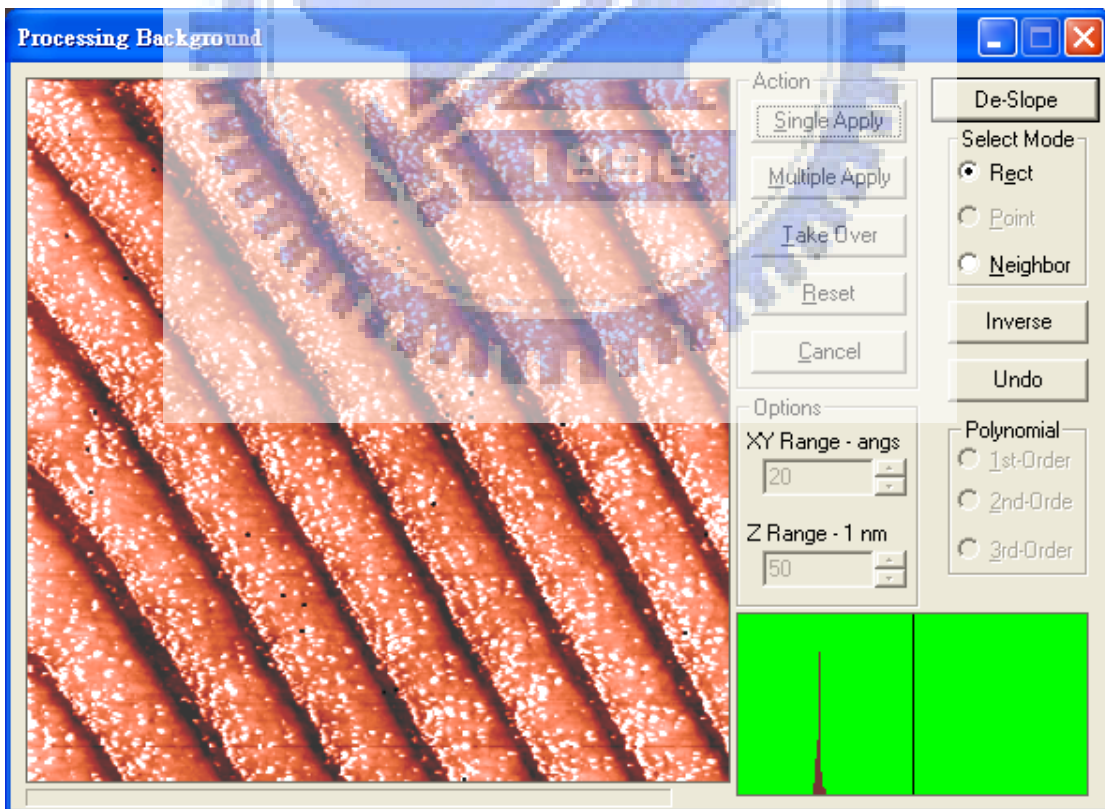


Fig.4.7 The image of DVD master surface taken by our simple STM.

Fig.4.7. is taken in a scan area of -10V ~ +10V we apply to the disk scanner. The

known periodic of the topography is 320 nm. So the disk scanner's piezo constant is about $3\mu\text{m}/20\text{V}=0.15\mu\text{m}/\text{V}$.

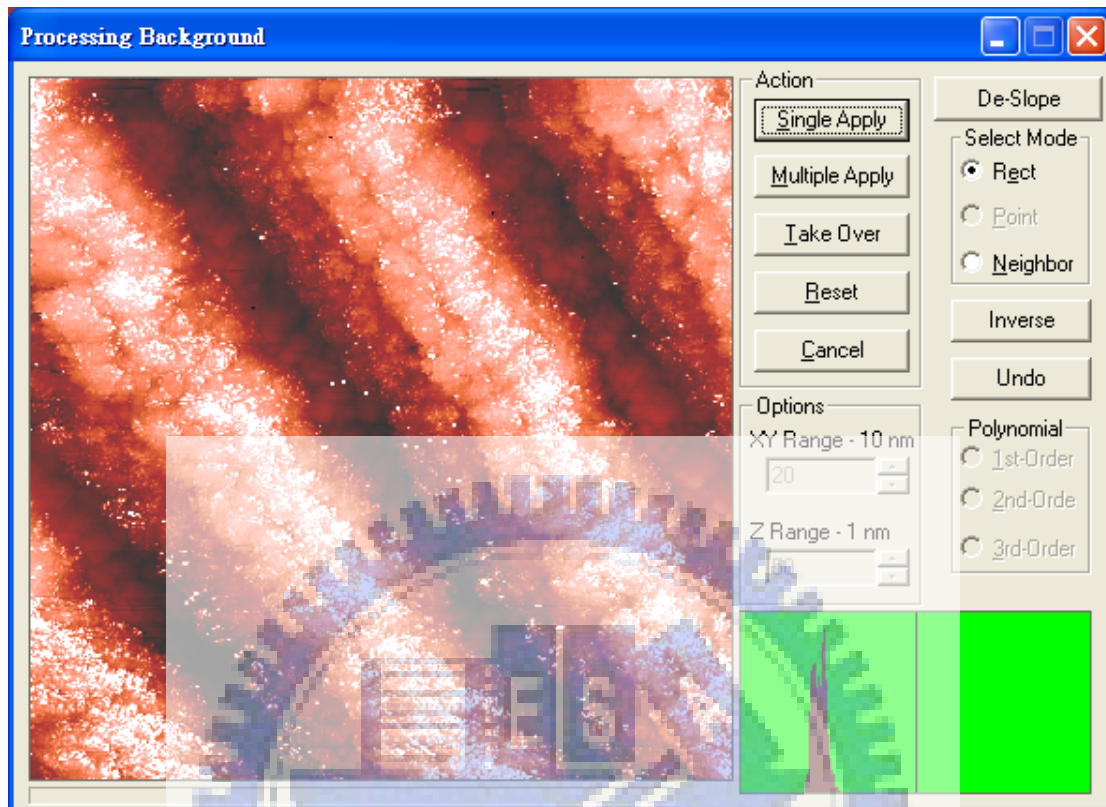


Fig.4.8. The image is taken in smaller scan area which means higher amplification.

Chapter 5 Conclusion

During the process of building the simple STM, we encountered many problems. The tip's approaching motion of our beginning design was not stable and not reversible. This causes the tip easily to crash into the sample. So the tip's condition would always be too bad to get a believable image. The control program also underwent many corrections and improvements to be suited to our STM. The problem of the tip's step motion can be solved by using a frame with high rigidity. And the ratio of the lever's arm should be larger enough to let the tip do micro-movement.

The noise in electric circuit is also bothersome. A metal box can shield the electronic elements from interference of electromagnetic waves. The thermal motion of electrons in electric elements can be reduce by lowering the manipulating temperature. In order to reduce the use of outer connecting wires, we do electronic layouts in one box. This also makes our instrument more compact.

The P-gain, I-gain values are important parameters when the system undergoes a feedback control. Since the feedback loop generally has some time delay, a high gain would mean a relatively fast approach of the reference position, while a low gain would mean a relatively slow approach. If the gain is set too high, the system will be corrected too quickly and too much, which will cause the system to oscillate around the reference point. If the gain is too low, the system will react too slowly to change the tip's height, which means the sample's topography is not well reflected. In theoretical PI-controller analysis, increasing P-gain would reduce the steady-state offset (but never reduce to zero) but lead to instability. Adding I-gain could eliminate the steady-state offset but let the transient response worse.

Reference

[1] Ref: C. J. Chen. *Introduction to Scanning Tunneling Microscopy*, Oxford, 1993.

[2] Ref: C. Kittel, *Introduction to Solid State Physics*, 7th edition, Wiley, 1996.

[3] Ref: 國立中興大學物理學研究所碩士學位論文-自製掃瞄式穿隧電流顯微鏡, 王雨瑞, 2005.

[4] Ref: A. I. Oliva, A. Romero G., J. L. Pena E. Anguiano and M. Aguilar, *Rev. Sci. Instrum.* 67(5), 1917 (1996).

